Surface Plasmon Enhancement of Two- and Three-Photon Absorption of Hoechst 33 258 Dye in Activated Gold Colloid Solution

Ion Cohanoschi and Florencio E. Hernández*

Department of Chemistry and School of Optics/CREOL/FPCE, University of Central Florida, P.O. Box 162366, Orlando, Florida 32816-2366

Received: February 21, 2005

Herein we present experimental evidence of the strong surface plasmon enhancement of two- and three-photon absorption of Hoechst 33 258 (2′-(4-hydrophenyl)-5-(4-methyl-1-piperazinyl)-2,5′-bis(1*H*-benzimidazole)) pentahydrate in an aqueous solution containing activated gold colloid. The 480-fold enhancement in two-photon absorption and 30-fold in three-photon absorption are predominantly attributed to the electric-field enhancement via surface plasmon resonance. The greater enhancement observed in two-photon absorption is due to the characteristic two- and three-photon absorption cross-sections of the dye.

1. Introduction

Two-photon absorption (2PA) is based on the simultaneous absorption of two photons in a single event.[1] A key feature of 2PA is an even-parity selection rule for symmetric molecules. Because the excitation probability for 2PA scales quadratically with the incident irradiance, the excitation is confined to the immediate vicinity of the focal plane of a focused light source. As a direct consequence, the spatial resolution is considerably increased,[2] and since there is usually no significant linear absorption outside the focal region, the penetration depth is much greater. Because two longer wavelength photons are needed, losses due to scattering are reduced.[3] This process has been widely used in two-photon confocal imaging.[4−6] Also, it has been recently tried in photodynamic therapy (PDT).[7−13] However, for more practical biomedical applications, there is still a great need of specifically designed molecules exhibiting stronger 2PA and/or higher order nonlinear absorption responses that afford greater penetration depth and spatial resolution.

Three-photon absorption (3PA) is an exciting possibility in biological imaging and phototherapy treatment that is still in its infancy.[14−17] The applicability of three-photon absorption processes is based on several key advantages: (a) improvement in penetration depth when working in the living organism transparency windows in the near-IR;[18] (b) minimization of loses due to scattering when longer wavelengths are used;[3] (c) enhancement of the spatial resolution.[2] Although 3PA seems to be a good candidate for biomedical applications, the rate of energy absorption for 3PA processes has a cubic dependence with the irradiance of the incident radiation.[19] Therefore, very high irradiance is required to induce three-photon excitations. At present, the only way to achieve such high irradiance is mainly by using sophisticated picosecond and femtosecond systems. This impediment has kept the scientific community from working more aggressively in this direction. Therefore, materials and processes that can overcome this limitation by lowering the irradiance requirement for 3PA may as well revolutionize the photonics field, creating unprecedented opportunities in biophotonics and nanophotonics.

The tactic that we propose to overcome the required high irradiances for multiphoton absorption of organic molecules is the use of the electric-field enhancement produced by the quantized oscillation of collective electrons in a plasma surface, i.e., surface plasmon.[20] This effect depends strongly on the type of metal, its size and shape, the incident wavelength, and the surrounding permittivity ϵ_m.[20] Theoretical calculations of the electric-field intensity enhancement through thin metal films, at 1100 nm (one of the living transparency windows),[18] predict a maximum enhancement of approximately 350-fold in Ag and 50 in Au.[20] Similar effects to those observed in metal nanolayers can be induced by metal nanoparticles. For instance, silver and gold spherical nanoparticles possess a very strong absorption band with maxima at ≈420 and ≈530 nm, respectively. These bands correspond to their surface plasmon resonance (SPR).[20] The two main advantages of using metal nanoparticles instead of metal films are the possibility to work in solutions and the tremendous concentration of the electric field (local-field enhancement).[20] Theoretical calculations carried out in metal nanospheres at 1100 nm show a maximum enhancement of the electric-field intensity of 1.1×10^5-fold in Ag and 2.0×10^3 in Au.[20]

Surface plasmon resonance has found many valuable applications in biophysics, biochemistry, and medicine through one-photon excitation fluorescence enhancement.[6,21−24] It has been demonstrated that the fluorescence quantum yield of a molecule can be improved to near unity when it is placed in the close vicinity of a thin metal layer.[24] The fluorescence quantum yield augmentation is caused by two main factors: electric-field enhancement and reduction of the fluorescence lifetime. Also, due to its tremendous electric-field enhancement, the SPR has been applied in nonlinear optics to second-harmonic generation (SHG),[25,26] Raman scattering,[27,28] amplification of light,[24] and more recently to 2PA processes.

Kano and Kawata[29] showed for the first time the possibility to enhance two-photon induced fluorescence by surface plasmon using the Kretschmann geometry.[30] By pumping at 800 nm, the authors[29] were able to demonstrate a fluorescence enhancement factor (FEF) ≈ 90 on LD490 dye-doped PMMA film deposited on a silver nanolayer. Later, Sanchez and co-workers showed

* To whom correspondence should be addressed.

10.1021/jp0508958 CCC: $30.25
Published on Web 07/13/2005

the possibility to do near-field fluorescence microscopy based on two-photon excitation with metal tips with an FEF 10 times greater than the one reported by Kano and Kawata.[31] Lakowicz et al. have also reported two-photon fluorescence enhancement from biochemical fluorophores in 1 μm thick samples placed between two quartz slides coated with silver islands.[32] The authors claimed 80-fold enhancement on their fluorophores via two-photon excitation. In Prasad's group two-photon emission enhancement using near-field probing surface plasmon was demonstrated. They reported an FEF $\approx$ 750 on doped organic nanoparticles adsorbed onto silver surfaces.[33] A surprising FEF $\geq$ 160 000 via 2PA was lately reported on thiol-chromophores attached to silver nanoparticle fractal clusters.[34] This extraordinary enhancement was attributed to a stronger electric-field enhancement via SPR accumulative effects in localized "hot spots".

So far, there is no experimental evidence of higher order excitation processes assisted by surface plasmon resonance. Also, most of the studies previously described have been done in doped polymeric films deposited on metal nanolayers or nanoparticles. More attractive biological and medical applications require multiphoton excitation enhancement via surface plasmon resonance in colloidal aqueous suspensions since water soluble molecules are more compatible with living systems.

In this article, we show the first experimental evidence of surface plasmon assisted three-photon absorption (3PA) enhancement in a Hoechst 33 258 pentahydrate (bis-benzimide) aqueous solution containing activated gold colloid. Also, two-photon absorption enhancement of this dye in a similar solution is demonstrated. Using open aperture Z-scan, we measured the two- and three-photon absorption coefficients of Hoechst 33 258/H_2O solutions in the absence and the presence of activated gold colloid. We demonstrate that the measured enhancement is a consequence of two different effects: the electric-field enhancement via surface plasmon resonance and the efficiency of the dye as a two- and three-photon absorber.

2. Experimental Section

2.1. Hoechst 33 258 Pentahydrate (Bis-benzimide). To decide which compound would allows us to demonstrate two- and three-photon absorption enhancement in aqueous solution using surface plasmon resonance, we considered three main features: (a) extended π-conjugation length to improve the nonlinear absorption;[35−38] (b) strong linear absorption between 250 and 400 nm to be able to induce 2PA and 3PA within the water nonabsorbing window; (c) water solubility. Hoechst 33 258 (2′-(4-hydrophenyl)-5-(4-methyl-1-piperazinyl)-2,5′-bis-(1*H*-benzimidazole)) pentahydrate, a commercial dye from Molecular Probes Inc., routinely used in common practice of visualization of DNA in gels[39,40] fulfills all these requirements. The molecular structure of this dye is shown at the top of Figure 1. Figure 1 also displays the linear absorption and emission spectra (excitation at 350 nm) of Hoechst 33 258 in aqueous solution at a concentration of 1×10^{-5} M. The measurements were carried out using an Agilent 8453 diode array UV−vis spectrophotometer and PTI Quanta-Master spectrofluorimeter, respectively (cell effects and solvent contribution were properly subtracted). Hoechst 33 258 presents high extinction coefficient (46 000 cm^{-1}) at 345.5 nm, fluorescence emission with maximum at 510 nm in water, and quantum yield $Q_f = 0.034$. The dye solution has no measurable absorption above 450 nm. Excitation beyond this wavelength can only occur through nonlinear processes. Also, the measured fluorescence anisotropy ($r = (I_{||} - I_{\perp})/(I_{||} + 2I_{\perp})$)[41] of the dye in glycerol at a concentration of 0.5×10^{-5} M is shown. The fluorescence anisotropy was obtained with the PTI Quanta-Master spectrofluorimeter upon excitation at 350 nm with linearly polarized light. The emission intensity was measured through a polarizer oriented parallel ($I_{||}$) and perpendicular ($I_{\perp}$) to the direction of the polarized excitation.[41] This curve reveals the spectral regions for the $S_0 \rightarrow S_1$ and $S_0 \rightarrow S_2$ transitions with maximum excitation at ca. 275 and 345 nm, respectively.

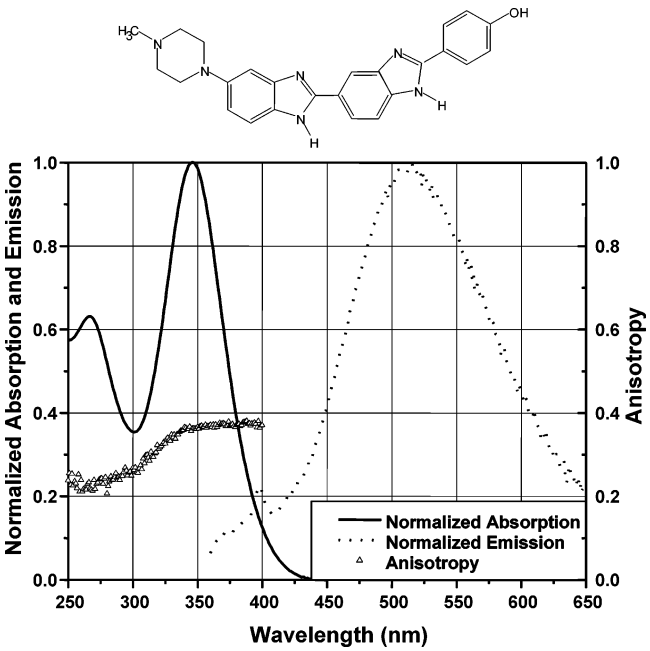

Figure 1. Molecular structure of Hoechst 33 258 (top). Normalized absorption (solid line) and normalized emission (dotted line) spectra of a 1×10^{-5} M Hoechst 33 258/H_2O solution (left side scale). Anisotropy curve (△) of a 0.5×10^{-5} M Hoechst 33 258/glycerol solution (right side scale).

2.2. Gold Nanoparticle Cluster Preparation and Characterization. Gold nanospheres of 16 nm average diameter (<15% size distribution) were synthesized with the wet chemical method of Turkevich et al.[42,43] Briefly, 50 mL of preboiled 2.5×10^{-4} M $AuHCl_4$ aqueous solution was mixed with 1.0 mL of 3.4×10^{-3} M sodium citrate solution. Then, this mixture was heated and stirred for 5 min. The deep red color of the solution revealed the presence of gold nanoparticles.[41,42] A typical surface plasmon resonance band with maximum at approximately 530 nm was observed using the Agilent 8453 spectrophotometer (see Figure 2). The nanoparticle size and distribution were determined by transmission electron microscopy (TEM) using an FEI Tecnai F30 TEM. Gold nanoparticles were mainly chosen because of their chemical stability in the presence of oxygen and water at room temperature.

To ensure 3PA enhancement using longer excitation wavelengths in the near-IR region, we employed a method commonly used in bulk surface enhanced Raman scattering (SERS), which consist on activating the metal colloid by electrolyte-induced aggregation.[44−46] Activated gold colloid (hot particles) was prepared by adding 0.5 mL of 1 M NaCl(aq) to 5.0 mL of the original gold nanoparticle solution. To determine whether the optically active hot particles were generated, we recorded a UV−vis absorption spectrum of the final solution 20 min after its preparation. In Figure 2 we show the typical broad absorption spectrum of activated gold colloid that extends to at least 1100 nm.[46] This effect is induced by the coupling of the individual dipole oscillators of the small isolated particles.[46] As a result

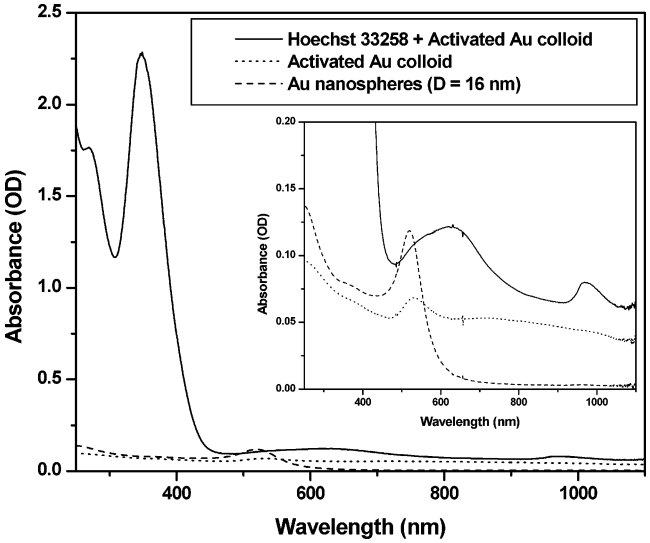

Figure 2. Absorbance vs wavelength of 16 nm diameter gold nanospheres (dashed line), activated gold colloid (dotted line), and Hoechst 33 258/H_2O solution (2.3×10^{-3} M) in the presence of activated gold colloid (solid line). The inset shows a closer view of the low absorbance region of the spectra.

normal modes of plasmon excitation that hold the cluster and cover a wide frequency region from the UV to the near-IR are generated.[46]

2.3. Hoechst 33 258 + Activated Gold Nanoparticle Colloid. Activated samples were prepared by mixing 0.5 mL of 1×10^{-2} M Hoechst 33 258/H_2O with 5.5 mL of the activated gold colloidal solution. The final concentration of Hoechst 33 258 in the activated solution was 8.3×10^{-4} M for 3PA and 1.4×10^{-3} M for 2PA. The absorption spectrum of the final mixture is shown in Figure 2. The dye in the presence of hot particles did not change its absorption spectrum. However, a background signal due to the presence of hot particles is observed. The inset in Figure 2 shows a closer view of the lower absorption region of the spectra. The SPR band of hot particles in Hoechst 33 258 solution is shifted to approximately 580 nm. This is an indication of dye molecules partially covering the hot particles. It is well-known that the position of the SPR band is very sensitive to ϵ_m.[20] The two bands with maxima at 620 and 980 nm suggest the generation of different shape clusters in the presence of the dye.[28]

Measurements of the pure dye were done on a Hoechst 33 258/H_2O solution at a final concentration 2.3×10^{-3} M. NaCl(aq) was also added to this pure dye solution to avoid matrix effects. The concentration of this solution was slightly greater than that with hot particles to ensure three-photon absorption of the dye in the absence of activated gold colloid.

2.4. Two- and Three-Photon Absorption Measurements. Two- and three-photon excitations were induced with a tunable OPG pumped by the third harmonic of a mode-locked, 25 ps full width at half-maximum (fwhm), Nd:YAG laser (EKSPLA), operating at a 10 Hz repetition rate. The beam was focused to 10.0 μm (HW1/e^{2}M) at 550 nm and 14.5 μm (HW1/e^{2}M) at 1064 nm with a 15 cm focal distance achromatic lens. The sample was held in a 1 mm path length quartz cell placed on a translation stage to scan it around the focal plane on the Z direction.

Using the well-known open aperture Z-scan technique,[47] we measured the two- and three-photon absorption coefficients of Hoechst 33 258/H_2O in the absence and the presence of hot particles. Because this method is very sensitive to the spatial beam intensity distribution, the beam was previously spatially filtered with a 100 μm diameter pinhole placed at the focal plane of a 20 cm focal distance achromatic plane-convex lens. A nearly Gaussian transverse intensity distribution, monitored with a Hitachi CCD camera was recovered.

To determine the two- and three-photon absorption coefficients, we fitted the experimental normalized transmittance vs Z (the sample cell position around the focal plane) using basic theoretical considerations for two- and three-photon absorption.[48] Neglecting linear absorption at the excitation wavelength, the relationship between the change in irradiance as a function of sample depth follows the equation

$$\frac{dI(z,r,t)}{dz} = -\alpha_n I(z,r,t)^n \tag{1}$$

where α_n is the absorption coefficient of nth order of the sample, at the wavelength of incident radiation. $I(z,r,t)$ is the irradiance that depends on the propagation distance within the sample z and the beam intensity radial (r) and temporal (t) distribution. For 2PA and 3PA, n is equal to 2 and 3, respectively. The general solution for this equation gives us the irradiance at the exit interface of the sample ($z = L$)

$$I(L,r,t) = \frac{I(z=0,r,t)}{\sqrt[n-1]{1 + (n-1)\alpha_n L I^{n-1}(z=0,r,t)}} \tag{2}$$

where $I(z=0,r,t)$ is the incident irradiance at the front side of the sample.

For pulses with temporal and spatial Gaussian profiles, eq 2 can be integrated in time and space and rearranged to obtain the normalized energy transmittance for two- and three-photon absorption in terms of the functions $X_n(x,Z)$ and $c_n(Z)$:

two-photon absorption

$$T_{2PA}(Z) = \frac{1}{\sqrt{\pi}\, c_2(Z)} \int_0^1 \frac{dx}{x\sqrt{-\ln x}} X_2(x,Z)$$

where

$$X_2(x,Z) = \ln\{1 + c_2(Z)x\}$$

$$c_2(Z) = \alpha_2\, I_0(Z)\, L$$

three-photon absorption

$$T_{3PA}(Z) = \frac{1}{\sqrt{\pi} c_3(Z)} \int_0^1 \frac{dx}{x\sqrt{-\ln x}} X_3(x,Z)$$

where

$$X_3(x,Z) = \ln\{c_3(Z)x + \sqrt{1 + c_3(Z)^2 x^2}\}$$

$$c_3(Z) = \sqrt{2\alpha_3\, I_0(Z)^2\, L} \tag{3}$$

In this equation, L is the distance traveled by the beam through the sample. The peak value of the incident irradiance $I_0(Z)$ at $z = 0$ can be estimated, for the different cell positions, using $w(Z) = w_0[1 + (Z^2/Z_0^2)]^{1/2}$, which yields $I_0(Z) = [2E_0/\pi\sqrt{\pi} t_p w(Z)^2]$.[3] E_0 is the pulse energy, t_p is the pulse width (HW1/eM), w_0 is the beam waist at focus (fwhm), $w(Z)$ is the radius of the beam at any position, Z_0 is the confocal parameter, and Z is the cell position with respect to the focal plane.

Relating α_n with the solute concentration d_0 (molarity) in solution and the photon energy $[h(c/\lambda)]$ of the incident radiation, we estimated the 2PA and 3PA cross-sections of the samples using eq 4 for each case:

two-photon absorption cross-section

$$\sigma_2' = \frac{\alpha_2}{10^{-3} N_A d_0}\left(\frac{hc}{\lambda}\right)$$

three-photon absorption cross-section

$$\sigma_3' = \frac{\alpha_3}{10^{-3} N_A d_0}\left(\frac{hc}{\lambda}\right)^2 \quad (4)$$

3. Results and Discussions

3.1. 2PA and 3PA Measurements of Pure Hoechst 33 258. The 2PA and 3PA coefficients of pure dye in a 2.3×10^{-3} M solution were measured using open aperture Z-scan.[47] On the basis of the anisotropy measurements, 2PA was excited at 550 nm ($S_0 \rightarrow S_2$) and 3PA at 1064 nm ($S_0 \rightarrow S_1$). These wavelengths correspond to the two- and three-photon absorption transitions with the highest probability.[19] Figure 3 shows the open aperture Z-scan curves and their corresponding to theoretical fittings at three different energies for 2PA (Figure 3a) and 3PA (Figure 3b) using eq 3. The average values of the 2PA and 3PA coefficients at their corresponding wavelengths were $\alpha_2 = (9.0 \pm 0.2) \times 10^{-11}$ cm²·W^{-1} and $\alpha_3 = (3.3 \pm 0.3) \times 10^{-22}$ cm³·W^{-2}. These coefficients yielded two- and three-photon absorption cross-sections $\sigma_2' = (2.4 \pm 0.2) \times 10^{-47}$ cm⁴·s·photon^{-1} and $\sigma_3' = (8.3 \pm 0.8) \times 10^{-78}$ cm⁶·s²·photon^{-2}. The high σ_2' and σ_3' of Hoechst 33 258 are attributed to the extended π-electron conjugation in the molecule.[38,48] The comparison of our results of pure Hoechst 33 258 σ_2' and σ_3' with our literature search[36−38,48−51] shows that this dye is a better two-photon absorber than a three-photon absorber. It has been demonstrated that while asymmetric charge transfer can confer high two-photon absorption cross-section to organic molecules with push−pull motif,[36−38] it decreases their three-photon absorption cross-section.[48,51] σ_3' is greater in molecules with symmetric charge transfer.[48]

3.2. 2PA and 3PA Measurements of Hoechst 33 258 in the Presence of Activated Au Colloid. Having characterized the pure dye, we measured the 2PA and 3PA coefficients of the Hoechst 33 258/H_2O solutions in the presence of activated gold colloid (α_n(+Au)). The excitation wavelengths for 2PA and 3PA were again 550 and 1064 nm, respectively. Figure 4 shows the open aperture Z-scan curves and their corresponding to theoretical fittings pumping at 550 nm (Figure 4a) and 1064 nm (Figure 4b) using eq 3. The measured 2PA and 3PA coefficients α_2(+Au) $= (2.7 \pm 0.2) \times 10^{-8}$ cm²·W^{-1} and α_3(+Au) $= (3.5 \pm 0.2) \times 10^{-21}$ cm³·W^{-2} yielded effective $\sigma_2' = (1160 \pm 0.2) \times 10^{47}$ cm⁴·s·photon^{-1} and σ_3'(+Au) $= (244 \pm 10) \times 10^{-78}$ cm⁶·s²·photon^{-2}, respectively. $\alpha_n(+Au)$ and $\sigma_n'(+Au)$ refer to the *n*th order absorption coefficients and cross-sections in the presence of activated gold colloid. Table 1 summarizes the absorption cross-sections for two- and three-photon absorption of Hoechst 33 258 in the absence and presence of gold hot particles.

The observed enhancement of the 2PA and 3PA of Hoechst 33 258 in the presence of gold hot particles is revealed through the absorption cross-sections ratio, $\sigma_n'(+\text{Au})/\sigma_n'$, in Table 1. Using open aperture Z-scan, we measured pure nonlinear absorption. Therefore, the achieved two- and three-photon absorption enhancement is mainly attributed to the electric-field intensity enhancement produced by the surface plasmon resonance. A contribution of additional relaxation mechanisms (radiative or nonradiative) to the total enhancement is not totally discarded. Molecules that can return faster to their ground state can experience more excitation−relaxation cycles in time.[24]

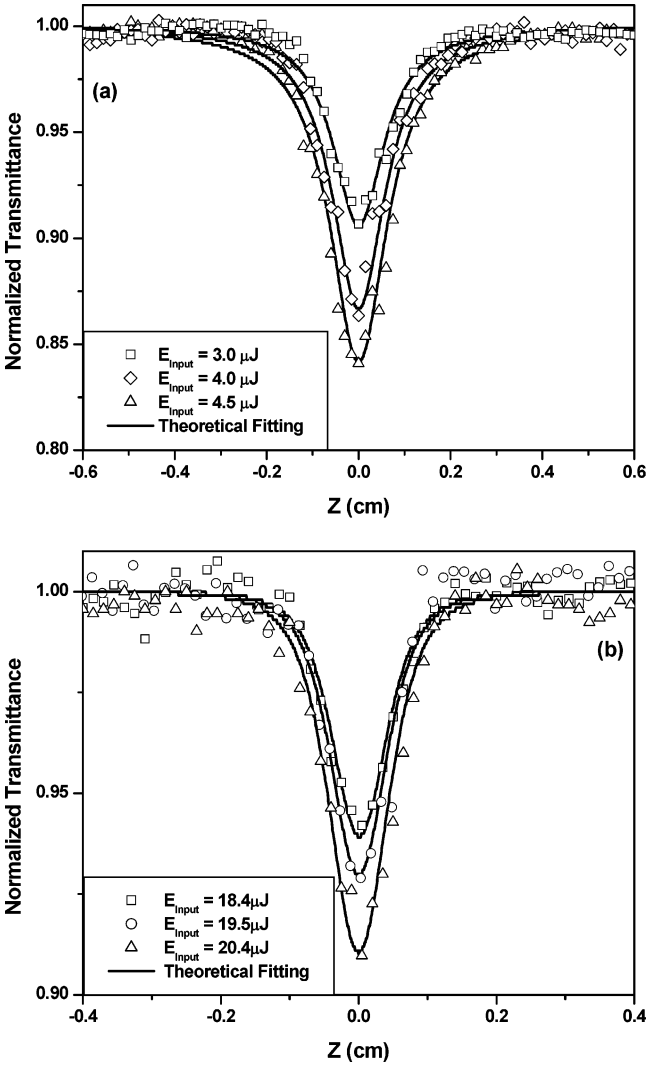

Figure 3. Open aperture Z-scan curves in Hoechst 33 258/H_2O solution (2.3×10^{-3} M) pumping at 550 nm (a) and 1064 nm (b). Solid lines are the best theoretical fittings using eq 3 for the change in transmittance for 2PA and 3PA. $w_0 = 10.0$ μm (HW1/e²M) at 550 nm and $w_0 = 14.5$ μm (HW1/e²M) at 1064 nm. 2PA and 3PA measurements were done at three different input energies (E_{in}): 3.0 (□), 4.0 (◇), and 4.5 μJ (△); 18.4 (□), 19.5 (○), and 20.4 μJ (△), respectively.

To reject any contribution to the nonlinear effect from hot particles,[52] we did measurements on pure activated gold colloid at 550 and 1064 nm. No change in transmission vs sample position at both excitation wavelengths was observed as shown in Figure 4. Therefore, changes in the transmission curves are merely produced by the dye.

2PA and 3PA enhancement was also attempted in Hoechst 33 258 in the presence of 16 nm diameter gold nanospheres that were not previously activated. No enhancement at all was observed. Stellacci and co-workers observed a similar effect on a self-assembly of two-photon chromophores on metal nanoparticles.[53]

3.3. Surface Plasmon Enhancement of 2PA vs 3PA in Hoechst 33 258. We report a 16-fold greater enhancement in 2PA compared to 3PA in Hoechst 33 258 (see Table 1). Figure

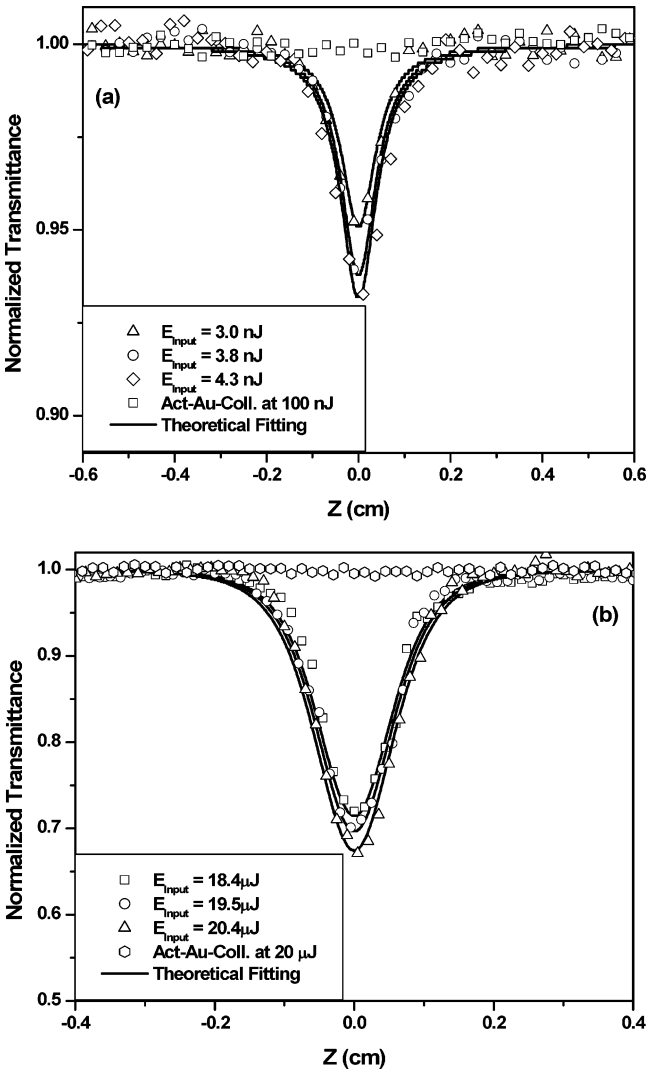

Figure 4. Open aperture Z-scan curves in Hoechst 33 258/H_2O solution in the presence of activated gold colloid, pumping at 550 nm (a) (8.3×10^{-4} M) and 1064 nm (b) (1.4×10^{-3} M). Solid lines are the best theoretical fittings using eq 3 for the change in transmittance for 2PA and 3PA. $w_0 = 10.0$ μm (HW1/e^2M) at 550 nm and $w_0 = 14.5$ μm (HW1/e^2M) at 1064 nm. 2PA and 3PA measurements were done at three different input energies (E_{in}): 3.0 (△), 3.8 (○), and 4.3 nJ (◇); 18.4 (□), 19.5 (○), and 20.4 μJ (△), respectively. In Figure 4a (□) corresponds to pure activated gold colloid pumping at 550 nm ($E_{in} =$ 100.0 nJ) and in Figure 4b (○) corresponds to pure activated gold colloid pumping at 1064 nm (($E_{in} = 20.0$ μJ).

5 shows the calculated maximum electric-field intensity enhancement (MEFIE) of gold nanospheres vs excitation wavelength.[20] These theoretical values were obtained by the sphere polarization formula in a uniform exterior field considering a complex refractive index (MEFIE $= |3\epsilon_r/\epsilon_{Im}|$).[20] The real ϵ_r and imaginary ϵ_{Im} part of the permittivity of gold at different wavelengths were obtained from Johnson and Christy's article.[54] According to Figure 5 the enhancement at 1064 nm ($MEFIE_{1064} \approx 2100$) should be approximately 21 times greater than that at 550 nm ($MEFIE_{550} \approx 100$).

Because the shape and the sizes of the activated gold nanoparticles are not precisely known,[28] and the theoretical model only applies to spherical nanoparticles,[20] the calculated $MEFIE_\lambda$ is not definitive. However, a greater enhancement for the longer wavelength should be expected because the imaginary part of the permittivity of gold is lower at 1064 nm than at 550 nm while its real part is greater (see Figure 5).[20]

TABLE 1

(a) Two-Photon Absorption Cross-Sections of Hoechst 33 258/H_2O in the Absence (σ_2') and in the Presence (σ_2'(+Au)) of Gold Hot Particles

λ (nm)	OAP[a]	σ_2' ($cm^4 \cdot s \cdot photon^{-1}$)	σ_2'(+Au) ($cm^4 \cdot s \cdot photon^{-1}$)	σ_2'(+Au)/σ_2'
550	2	$(2.4 \pm 0.2) \times 10^{-47}$	$(1160 \pm 0.2) \times 10^{-47}$	≈480

(b) Three-Photon Absorption Cross-Sections of Hoechst 33 258/H_2O in the Absence (σ_3') and Presence (σ_3'(+Au)) of Gold Hot Particles

λ (nm)	OAP[b]	σ_3' ($cm^6 \cdot s^2 \cdot photon^{-2}$)	σ_3'(+Au) ($cm^6 \cdot s^2 \cdot photon^{-2}$)	(σ_3'(+Au))/(σ_3')
1064	3	$(8.3 \pm 0.8) \times 10^{-78}$	$(244 \pm 10) \times 10^{-78}$	≈30

[a] Order of the absorption process, OAP. 2PA cross-section values and standard deviations correspond to the average of three single measurements taken for three different energies. [b] Order of the absorption process, OAP. 3PA cross-section values and standard deviations correspond to the average of three single measurements taken for three different energies.

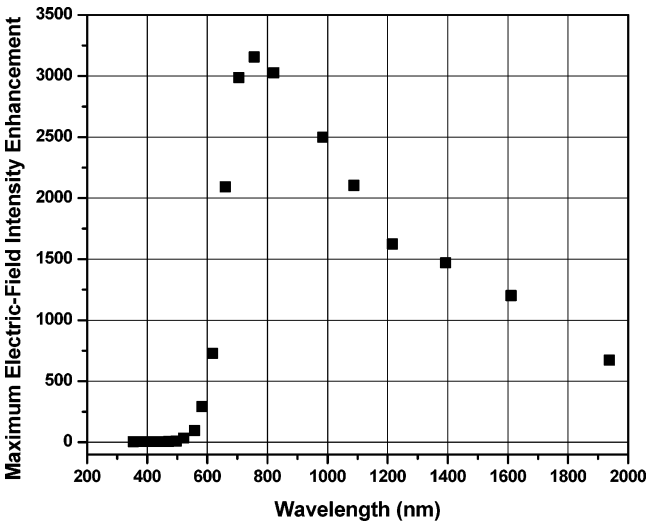

Figure 5. Theoretical maximum electric-field intensity enhancement (MEFIE) vs wavelength for spherical nanoparticles. MEFIE $= 3\epsilon_r^2/\epsilon_{Im}^2$, where ϵ_r and ϵ_{Im} are the real and imaginary part of the permittivity of gold, respectively.[20,52]

It is know that the transition probability of two- and three-photon processes presents a quadratic and a cubic dependence with irradiance, respectively. Therefore, higher irradiance is required for 3PA than 2PA, since σ_2' is always much greater than σ_3'.[38,48] Thus 3PA could be considered less sensitive to the electric-field enhancement via SPR than 2PA.

The comparison of our results of pure Hoechst 33 258 σ_2' and σ_3' with our literature search in section 3.1 revealed that Hoechst 33 258 is a better two-photon absorber than it is a three-photon absorber. In Figure 6 we show the experimental and calculated normalized transmittance vs irradiance of Hoechst 33 258. We used our experimental parameters and the measured two- and three-photon absorption coefficients of the dye. Comparing the normalized transmittance vs irradiance of 2PA and 3PA, one can notice that the irradiance corresponding to the starting point of 2PA of Hoechst 33 258 is at least 10 times lower than that of 3PA. For this reason, 2PA is more sensitive to electric-field intensity enhancement than 3PA in the lower irradiance region, i.e., below $\approx 1 \times 10^{11}$ W/cm^2. At higher irradiance, i.e., above $\approx 1 \times 10^{11}$ W/cm^2, the normalized transmittance of 3PA decreases faster than that of 2PA as expected.[3] Consequently, 3PA is more sensitive to electric-field

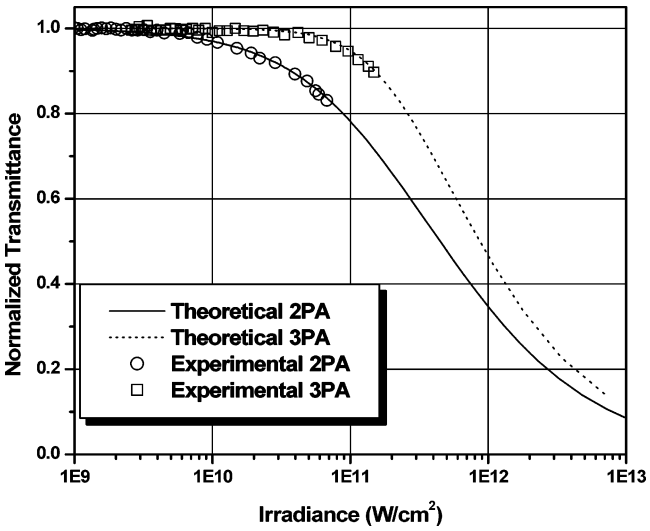

Figure 6. Experimental normalized transmittance vs input irradiance (W/cm^2) of pure Hoechst 33 258/H_2O for 2PA (○) and 3PA (□), and their corresponding theoretical values for 2PA (solid line) and 3PA (dotted line). The theoretical data were determined using the experimental parameters and the measured 2PA and 3PA coefficients $\alpha_2 = (9.0 \pm 0.2) \times 10^{-11}$ cm²·W^{-1} and $\alpha_3 = (3.3 \pm 0.3) \times 10^{-22}$ cm³·W^{-2}.

intensity enhancement once it gets initiated. To preserve the integrity of our cell, we avoided measurements at higher irradiance values.

4. Conclusions

Hoechst 33 258 presents high two- and three-photon absorption cross-sections. In the presence of activated gold colloid, the two- and three-photon absorptions of Hoechst 33 258 are enhanced by 480- and 30-fold, respectively. This is a direct consequence of the electric-field enhancement generated by the surface plasmon on activated gold colloid. Activated gold colloid is vital for 2PA and 3PA enhancement as it is for SERS. The efficiency of multiphoton absorption enhancement via surface plasmon resonance strongly depends on the multiphoton absorption cross-sections of the chromophore. This observation has to be carefully considered when reporting surface plasmon enhanced multiphoton absorption in molecular probes. The disparity observed among literature values of surface plasmon enhancement of 2PA has long been attributed to the experimental geometry, the nanostructure composition, size, and shape. Our results demonstrate that the existent discrepancy might have been also originated by the differences in the multiphoton absorption cross-section of the different dyes.

Acknowledgment. This research was supported by start up funds provided to F.E.H. by the Department of Chemistry, University of Central Florida, and the In-House Research Award (#11649003), UCF. The authors acknowledge Dr. Simeonson (Advanced Monitoring, Inc.) and Prof. Lopéz-Quintela (Universidade de Santiago de Compostela, Spain) for their valuable scientific input in sample preparations.

References and Notes

(1) Goeppert-Mayer, M. *Ann. Phys.* **1931**, *9*, 273−294.
(2) Min, G. *Opt. Lett.* **1996**, *21*, 988−990.
(3) Boyd, R. W. *Nonlinear Optics*; Academic Press: San Diego, CA, 1992; Chapters 4 and 8.
(4) Denk, W.; Strickler, J. H.; Webb, W. W. *Science* **1990**, *248*, 73−76.
(5) Larson, D. R.; Zipfel, W. R.; Williams, R. M.; Clark, S. W.; Bruchez, M. P.; Wise, F. W.; Webb, W. W. *Science* **2003**, *300*, 1434−1436.
(6) Squirel, J. M.; Wokosin, D. L.; White, J. G.; Bavister, B. D. *Nat. Biotechnol.* **1999**, *17*, 763−767.
(7) Karotki, A.; Drobizhev, M. A.; Kurk, M.; Rebane, A.; Nickel, E.; Spangler, C. W. *Proc. SPIE−Int. Soc. Opt. Eng.* **2002**, *4612*, 143−151.
(8) Madsen, S. J.; Sun, C.; Tomberg, B. J.; Wallace, V. P.; Hirschberg, H. *Photochem. Photobiol.* **2000**, *72*, 128−134.
(9) Wachter, E. A.; Partridge, W. P.; Fisher, W. G.; Dees, H. C.; Petersen, M. G. *Proc. SPIE−Int. Soc. Opt. Eng.* **1998**, 68−75.
(10) Frederiksen, P. K.; Jorgensen, M.; Ogilby, P. R. *J. Am. Chem. Soc.* **2001**, *123*, 1215−1221.
(11) Fisher, W. G.; Partridge, W. P.; Dees, C., Jr.; Wachter, E. A. *Photochem. Photobiol.* **1997**, *66*, 141−155.
(12) Poulsen, T. D.; Frederiksen, P. K.; Jorgensen, M.; Mikkelsen, K. V.; Ogilby, P. R. *J. Phys. Chem.* **2001**, *105*, 11488−11495.
(13) Bhawalkar, D.; Kumar, N. D.; Zhao, C. F.; Prasad, P. N. *J. Clin. Laser Med. Surg.* **1997**, *15*, 201−204.
(14) Gryczynski, I.; Gryczynski, H.; Malak, M.; Schrader, P.; Engelhardt, H.; Kano, H.; Hell, S. W. *Biophys. J.* **1997**, *72*, 567−578.
(15) Hell, S. W.; Bahlmann, K.; Schrader, M.; Soini, A.; Malak, H.; Gryczynski, I.; Lakowicz, J. R. *J. Biomed. Opt.* **1996**, *1*, 71−74.
(16) Szmacinski, H.; Gryczynski, I.; Gryczynski, I. *Biophys. J.* **1996**, *70*, 547−555.
(17) Maiti, S.; Shear, J. B.; Williams, R. M.; Zipfel, W. R.; Webb, W. W. *Science* **1997**, *275*, 530−532.
(18) Attas, E. M.; Sowa, M. G,; Posthumus, T. B.; Schattka, B. J.; Mantsch, H. H.; Zhang, S. L. L. *Biopolymers* **2002**, *67*, 96−106.
(19) Friedrich, D. M. *J. Chem. Phys.* **1981**, *75*, 3258−3268.
(20) Heinz, R. *Surface Plasmons on smooth and rough Surfaces and on Grattings*; Springer-Verlag: New York, 1988.
(21) Liedberg, B.; Nylander, C.; Lundstrom, I. *Biosens. Bioelectron.* **1995**, *10*, R1−R9.
(22) Libermann, T.; Knoll, W. *Colloids Surf., A* **2000**, *171*, 115−130.
(23) Campbell, B.; Lei, J.; Kiaei, D.; Sustarsic, D.; El Shami, S. *Clin Chem.* **2004**, *50*, 1942−1943.
(24) Lakowicz, J. R. *Anal. Biochem.* **2001**, *298*, 1−24.
(25) Chen, C. K.; de Castro, A. R. B.; Chen, Y. R. *Phys. Rev. Lett.* **1981**, *46*, 145.
(26) Wokaun, A.; Bergman, J. G.; Heritage, J. P.; Glass, A. M.; Liao, P. F.; Olson, D. H. *Phys. Rev. B* **1981**, *24*, 849.
(27) Otto, A.; Mrozek, I.; Grabhorn, H.; Akemann, W. *J. Phys. Condens. Mater.* **1992**, *4*, 1143−1212.
(28) Nie, S.; Emory, S. R. *Science* **1997**, *275*, 1102−1106.
(29) Kano, H.; Kawata, S. *Opt. Lett.* **1996**, *21*, 1848−1850.
(30) Kretschmann, E. *Z. Phys.* **1971**, *241*, 313−&.
(31) Sánchez, E. J.; Novotny, L.; Xie, X. S. *Phys. Rev. Lett.* **1999**, *82*, 4014−4017.
(32) Gryczynski, I.; Malicka, J.; Shen, Y.; Gryczynski, Z.; Lakowicz, J. R. *J. Phys. Chem. B* **2002**, *106*, 2191−2195.
(33) Shen, Y.; Swiatkiewicz, J.; Lin, T.-C.; Markowicz, P.; Paras, N. P. *J. Phys. Chem. B* **2002**, *106*, 4040−4042.
(34) Wenseleers, W.; Stellacci, F.; Meyer-Friedrichsen, T.; Mangel, T.; Bauer, C. A.; Pond, S. J. K.; Marder, S. R.; Perry, J. W. *J. Phys. Chem. B* **2002**, *106*, 6853−6863.
(35) Perry, J. W.; Mansour, K.; Lee, J. Y. S.; Xu, X. L.; Bedwhorth, P. V.; Chen, C. T.; Ng, D.; Marder, S. R.; Miles, P.; Wada, T.; Tian, M.; Sasabe, H. *Science* **1996**, *273*, 1533−1536.
(36) Kogej, T.; Beljonne, D.; Meyers, F.; Perry, J. W.; Marder, S. R.; Bredas, J. L. *Chem. Phys. Lett.* **1998**, *298*, 1−6.
(37) Reinhard, B.; Brott, L. L.; Clarson, S. J.; Dillard, A. G.; Bhatt, J. C.; Kannan, R.; Yuan, L.; He, G. S.; Prasad, P. N. *Chem. Mater.* **1998**, *10*, 1863−1874.
(38) Albota, M.; Beljonne, D.; Bredas, J. L.; Ehrlich, J. E.; Fu, J. Y.; Heikal, A. A.; Hess, S. E.; Kogej, T.; Levin, M. D.; Marder, S. R.; McCord-Maughon, D.; Perry, J. W.; Rockel, H.; Rumi, M.; Subramaniam, G.; Webb, W. W.; Wu, X. L.; Xu, C. *Science* **1998**, *281*, 1653−1656.
(39) Leatherbarrow, E. L.; Jenner, T. J.; O'Neill, P.; Botchway, S. W.; Conein, E.; Gaur, V.; Parker, A. W. *Laser of Science Facility Prog.−Biology* **2003**, 144−146.
(40) http://www.turnerbiosystems.com/doc/appnotes/998_7074.html.
(41) Lakowicz, J. R. *Principles of fluorescence Spectroscopy*, 2nd ed.; Kluwer Academic: New York, 1999.
(42) Turkevich, J.; Stevenson, P. C.; Hiller, J. *Discuss. Faraday Soc.* **1951**, *11*, 55
(43) Frens, G. *Nat. Phys. Sci.* **1973**, *241*, 20.
(44) Schatz, G. *Acc. Chem. Res.* **1984**, *17*, 370.
(45) Moskovits, M. *Rev. Mod. Phys.* **1985**, *57*, 783.
(46) Shalaev, V. M. *Phys. Rep.* **1996**, *272*, 61−137.
(47) Sheik-Bahae, M.; Said, A. A.; Wei, T.; Hagan, D. J.; Van Stryland, E. W. *IEEE J. Quantum Electron.* **1990**, *26*, 760.

(48) Hernández, F. E.; Belfield, K. D.; Cohanoschi, I. *Chem. Phys. Lett.* **2004**, *391*, 22−26.
(49) Belfield, K. D.; Morales, A. R.; Kang, B. S.; Hales, J. M.; Hagan, D. J.; Van Stryland, E. W.; Chapela, V. M.; Percino, J. *Chem. Mater.* **2004**, *16*, 2267−2273.
(50) Zhang, J.; Cui, Y.; Wang, M.; Xu C.; Zhong, Y.; Liu, J. *Chem. Lett.* **2001**, 824−825.
(51) Hernández, F. E.; Belfield, K. D.; Cohanoschi, I.; Balu, M.; Schafer, K. J. *Appl. Opt.* **2004**, *43*, 5394−5398.
(52) Bloemer, M. J.; Haus, J. W.; Ashley P. R. *J. Opt. Soc. Am. B* **1990**, *7*, 790−795.
(53) Stellacci, F.; Bauer, C. A.; Meyer-Friedrichsen, T.; Wenseleers, W.; Marder, S. R.; Perry J. W. *J. Am. Chem. Soc.* **2003**, *125*, 328−329.
(54) Johnson, P. B.; Christy, R. W. *Phys. Rev. E* **1992**, *6*, 4370−4379.